Supporting Information: Probing the Spin Spiral in Fe Chains on Ir(001) using Magnetic Exchange Force Microscopy

Yuuki Adachi, Yuuki Yasui, Atsushi Iiyama, Wataru Kurahashi, Rihito Nagase, and Yoshiaki Sugimoto*

Department of Advanced Materials Science, The University of Tokyo, Kashiwa, Chiba 277-8561, Japan

E-mail: ysugimoto@k.u-tokyo.ac.jp

Materials and method

The experiments were conducted using a custom-built scanning probe microscope operating under ultra-high vacuum conditions at 4.5 K.[S1] A commercial quartz length-extension resonator (LER), known as a Kolibri sensor provided by SPECS, equipped with a tungsten (W) tip, was utilized. The microscope is a combined AFM and STM system capable of applying high magnetic fields of up to 11 T perpendicular to the surface. The oscillation amplitude is $A \sim 120\,\mathrm{pm}$. For differential conductance ($\mathrm{d}I/\mathrm{d}V$) spectroscopy, we employed a lock-in technique with a modulated sample bias voltage of 100 mV at 777 Hz. The experiments were carried out with magnetic fields ranging from 0 T to 11 T. The Ir(001) surface was prepared by Ar^+ ion sputtering followed by annealing at 1000 °C under oxygen exposure of approximately 2.0×10^{-7} torr and subsequently annealed at 1200 °C for 10 s. To fabricate the Fe chain on Ir(001), less than 20 % to 25 % of a monolayer of Fe was deposited onto the clean Ir(001) surface at room temperature.[S2–S5]

The bi-atomic Fe chain on Ir(001)

The bi-atomic Fe chain on Ir(001) serves as a model system exhibiting a spin spiral state within a one-dimensional nanostructure.[S2,S3,S6] This spin spiral arises due to the competition between direct exchange interactions and Dzyaloshinskii–Moriya (DM) interactions, leading to the formation of nonlinear spins along the chain axis. Consequently, vector spin chirality is defined by the cross product of the spin vectors of neighboring nonlinear spins, resulting in a topologically protected spin structure within the chain.[S7] In finite chains, the application of an external magnetic field locks the spin spiral in real space through the alignment of the end spins.

Definition of tip-sample distances

The tip–sample distances in Figure 3, Figure 4, Figure S5 and Figure S6 are same so that the z_{d} can be directly compared. The topographic height of z in other Figures are different so that they cannot be directly compared. The black dotted line in Figure 3a of the main text was obtained by extracting the decay length κ from the tunneling current (I), using the equation $a\exp(-\kappa z_{\mathrm{d}})$, where a is free parameter.

Picking up Fe atoms from the surface

In our experiment, the fabrication of the magnetic tip was carried out as follows: First, the adsorption position of the target Fe chain was confirmed using STM imaging with a tungsten (W) tip. After acquiring the STM image, the W tip was carefully positioned above a different Fe chain, and the feedback loop was turned off. The W tip was then vertically approached approximately 1.3 nm to the Fe chain to pick up Fe atoms onto the tip apex. Subsequently, the target Fe chain was scanned to verify the formation of the stable Fe tip. This procedure was typically repeated several times to ensure a stable Fe tip. Figures S1a–S1d illustrate an example of the Fe atom pick-up process from the Fe chain. Initially, we scanned the target Fe chain using a W tip (Figure S1a). Next, the W tip was positioned above a different, smaller Fe chain (highlighted by the white circle in Figure S1b) and gently moved into the chain by approximately 1.3 nm from the STM set point. The slight deformation of the smaller Fe chain, as shown in Figures S1c and S1f, indicates that several Fe atoms were attached to the tip apex. Finally, we rescanned the target Fe chain to confirm the appearance of magnetic contrast along the Fe chain (Figures S1d and S1e). Therefore, a stable spin-polarized tip can be reliably prepared by picking up Fe atoms from the surface.

SP-STM images of the different length of the Fe chains on Ir(001)

Figure S2a presents a large-area spin-polarized scanning tunneling microscopy (SP-STM) image obtained in constant current mode. In this image, single strands of varying lengths, corresponding to bi-atomic Fe chains located in the trenches, can be observed. An external magnetic field of $-4.0\,\mathrm{T}$ was applied, resulting in maxima and minima along the Fe chain axis that indicate the positions where the magnetization components point either downward or upward within the spin spiral. Some Fe chains in the SP-STM image, highlighted by the pink rectangle, exhibit reduced magnetic corrugation, suggesting that the strength of magnetic corrugation varies between chains (while the green rectangle indicates the Fe chain with stronger corrugation). Similar observations have been reported in previous studies, where these variations were attributed to parity effects caused by the finite lengths of the Fe chains.[S3,S6] Thus, we successfully measured the net magnetic moment of the spin spiral in the Fe chain using the magnetic tip. Figures S2c and S2d were acquired using the same scanning parameters, but with an increased external magnetic field of up to $-11\,\mathrm{T}$. A similar trend in the magnetic contrast was observed in the Fe chain, as depicted in Figure S2d.

SP-STM image of the Fe chain taken at different bias voltage

To characterize the Fe chain using the magnetic tip, the bias voltage dependence of the tunneling current (I) and conductance ($\mathrm{d}I/\mathrm{d}V$) was simultaneously recorded by fixing the tip on the bright and dark regions of the Fe chain in the SP-STM image (see inset in Figure S3a). In Figure S3a, both I and $\mathrm{d}I/\mathrm{d}V$ exhibit weak contrast at negative bias, but strong contrast at positive bias. This observation is further supported by the SP-STM images obtained at different bias voltages, as shown in Figures S3b–S3e. Notably, in Figures S3b–S3d, the lateral positions of the maxima and minima along the chain axis in $z(x)$ remain almost identical, despite variations in the positive bias voltage set points. These results suggest that the observed contrast is primarily due to a magnetic origin, ruling out the possibility of a standing wave effect, which is often seen in quantum well structures of one-dimensional systems.[S8,S9] When the bias voltage was set to a negative value, the SP-STM image showed barely any contrast, as seen in Figure S3e.

SP-STM image of the Fe chain taken at different external magnetic fields

Figures S4(a–d) and S4(e–h) present the SP-STM images of the same Fe chain acquired at different external magnetic fields, and their corresponding line profiles. To quantify the strength of the magnetic corrugation, we plotted the normalized average strength of the magnetic corrugation in the Fe chain, as shown in Figure S4i. The average magnitude of the magnetic corrugation at each magnetic field was normalized by dividing it by the average magnitude of the magnetic corrugation at 9.0 T. In Figure S4i, the normalized magnetic contrast increases monotonically with the external magnetic field. Previous research shows that magnetic contrast increases monotonically with the external magnetic field up to 4.0 T.[S10] Figure S4i shows a monotonic increase in magnetic contrast with the external magnetic field up to 9.0 T. Additionally, we confirm the magnetic contrast of Fe chain at -11 T in Figure S2c. These findings indicate that the spin spiral is robust against the external magnetic field within the measured range.

Tip-sample distance dependence of short-range forces and potential energy

To quantify the short-range forces, we measured the tip-sample distance dependence of the frequency shift, Δf, as the Fe tip approached the Fe chain ($\Delta f_{\mathrm{Fe\,chain}}$) and the Ir surface ($\Delta f_{\mathrm{Ir}}$), as shown by the black and green curves in Figure S5a. Subsequently, the two Δf curves were subtracted to extract the short-range frequency shift, Δf_{SR} (z_{d}), between the Fe chain atom and the Fe tip. This calculation is given by $\Delta f_{\mathrm{SR}}\,(z_{\mathrm{d}}) = \Delta f_{\mathrm{Fe\,chain}}\,(z_{\mathrm{d}}) - \Delta f_{\mathrm{Ir}}\,(z_{\mathrm{d}})$, as represented by the red curve in Figure S5a. The results in Figure S5a indicate that Δf_{SR} (z_{d}) decreases monotonically as the tip approaches the surface. The short-range force, F_{SR} (z_{d}), was derived from Δf_{SR} (z_{d}) using the Sader formula,[S11] as shown in Figure S5b. An enlarged view of these data is provided in Figure 3c. The potential energy, U (z_{d}), was then obtained by integrating F_{SR} (z_{d}) with respect to the z_{d} direction, as displayed in Figure S5c, with an enlarged view in Figure 3d.

Full data sets of MExFM and SP-STM images of the Fe chain

Figure S6(a-j) presents the complete data sets corresponding to Figure 4 in the main text. Figure S6a displays the SP-STM image of the Fe chain obtained in constant current mode, along with the corresponding line profile. The image is taken under an upward external magnetic field of 3.0 T, thus, the maxima and minima along the Fe chain indicate positions where the magnetization components point upward or downward within the spin spiral. Following the STM imaging, the tip was positioned above the Fe chain, and the z-feedback was turned off. The tip was then vertically approached to the Fe chain, and scanning was performed in constant height mode, as illustrated in Figure S6b.

To qualitatively assess the dominant effects of magnetic and chemical contrasts in the line profile, we present normalized $\Delta f(x)$ and $I(x)$ in Figure S6b, where $\Delta f_{\text{normalized}}(x) = \Delta f(x)/\Delta f_{\text{Fe chain}}$ and $I_{\text{normalized}}(x) = I(x)/I_{\text{Fe chain}}$. Here, $\Delta f_{\text{Fe chain}}$ and $I_{\text{Fe chain}}$ correspond to the average values of Δf and I at $2.0\,\text{nm} \leq x \leq 7.2\,\text{nm}$. In Figure S6b, we observe a slight decrease in $\Delta f(x)$, which can be attributed to the long-range van der Waals interaction between the tip and the Fe chain on the Ir surface.

We subsequently repeated the scanning by varying the tip-sample distance, as depicted in Figures S6(c-j). At larger tip-sample distances, shown in Figures S6(c) and (d), corrugation in $\Delta f_{\text{normalized}}(x)$ along the Fe chain is evident. As we discussed in the main text, the lateral position of the minima and maxima in $\Delta f_{\text{normalized}}(x)$ agrees well with the lateral position of the maxima and minima in $I_{\text{normalized}}(x)$. Therefore, we conclude that the corrugation observed in $\Delta f_{\text{normalized}}(x)$ originates from the ferromagnetic coupling between the spin spiral and the Fe tip. At medium tip-sample distances, shown in Figures S6(e-g), a magnetic contrast is observed in $I_{\text{normalized}}(x)$, attributed to the spin spiral. At smaller tip-sample distances, as illustrated in Figures S6(h-j), we observe a chemical contrast in $\Delta f_{\text{normalized}}(x)$ along the Fe chain. The periodicity of this modulation is approximately 0.27 nm, which is consistent with previous theoretical results.[S12] At small tip-sample distances, $I_{\text{normalized}}(x)$ exhibits both magnetic and chemical contrasts. We have performed fast Fourier transform (FFT) to analyze the MExFM images (not shown). However, we hardly observe a signal for the spin spiral in those FFT results, which may be due to the short length of the Fe chain.

Reproducibility of the ferromagnetic coupling between Fe tip and Fe chain

In this section, we demonstrate the reproducibility of ferromagnetic coupling and atomic resolution using MExFM and SP-STM techniques. Figure S7a presents the SP-STM image of the Fe chain obtained in constant current mode. The image is taken under an upward external magnetic field of 3.0 T, thus the maxima and minima along the Fe chain axis indicate positions where the magnetization components point upward or downward relative to the surface, as shown in the line profile of Figure S7d. Subsequently, we switched to constant height mode to perform MExFM and SP-STM on this chain. Figures S7(b, c) and S7e illustrate the Δf and tunneling current images, accompanied by the corresponding line profiles. In Figure S7e, we display normalized $\Delta f(x)$ and $I(x)$, defined as $\Delta f_{\text{normalized}}(x) = \Delta f(x)/\Delta f_{\text{Fe chain}}$ and $I_{\text{normalized}}(x) = I(x)/I_{\text{Fe chain}}$. Here, $\Delta f_{\text{Fe chain}}$ and $I_{\text{Fe chain}}$ correspond to the average values of Δf and I at $2.0\,\text{nm} \leq x \leq 6.0\,\text{nm}$. Focusing on $\Delta f_{\text{normalized}}(x)$ in Figure S7e, we observe that the distance between small corrugations is approximately 0.27 nm, indicating a chemical contrast. Moreover, the lateral position of the minima associated with the large corrugation (indicated by a dotted line across Figures S7(a-e)) in $\Delta f_{\text{normalized}}(x)$ aligns well with the lateral position of the maxima in the tunneling current (blue curve in Figure S7e). This observation suggests that the $\Delta f_{\text{normalized}}$ contrast arises from ferromagnetic coupling, which intensifies with the alignment of spins at the tip apex and the spins in the Fe chain, producing the corresponding features in $\Delta f_{\text{normalized}}(x)$. Notably, the distance between the maxima in the large corrugation is approximately 1.01 nm, which is incommensurate with the length of three atomic lengths ($1.01\,\text{nm} = 0.27\,\text{nm} \times 3.7$). Such incommensurability has also been observed in nano-skyrmion surfaces.[S13] Therefore, we confirm the reproducibility of MExFM and SP-STM measurements on the Fe chain.

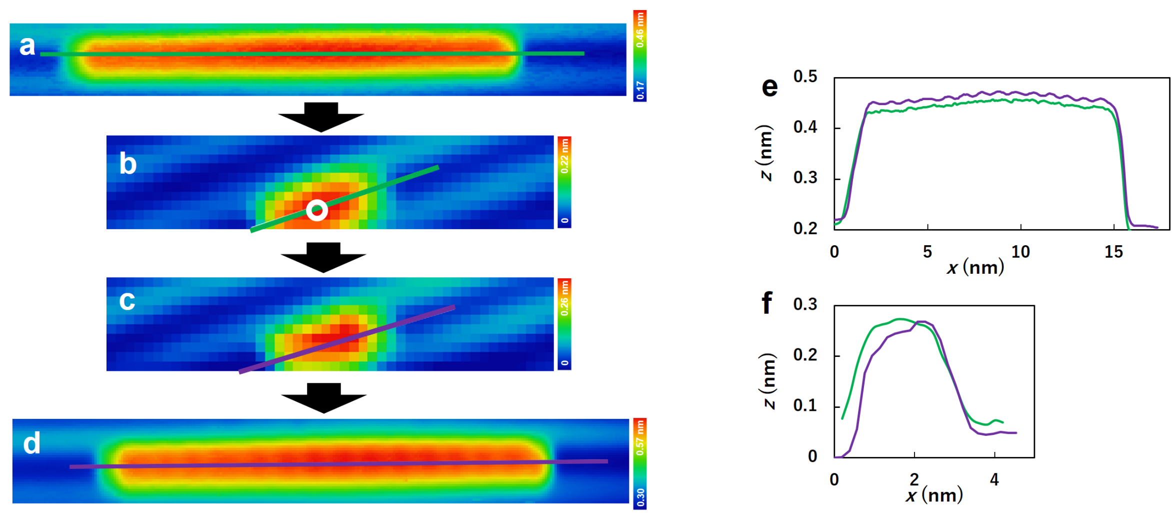

Figure S1: (a-d) Consecutive STM topography image Fe chain on Ir(001). Imaging condition: Constant current mode. $V = 500\,\mathrm{mV}$, $T = 4.5\,\mathrm{K}$, $B = 2.0\,\mathrm{T}$. (a,d) $I = 1.0\,\mathrm{nA}$; (b,c) $I = 50\,\mathrm{pA}$. (e,f) Topographic line profile obtained from the target Fe chain (a,d) and small Fe chain (b,c). The position of the profile is indicated by different colors in (a-d). Tip position is indicated by a white circle in (b).

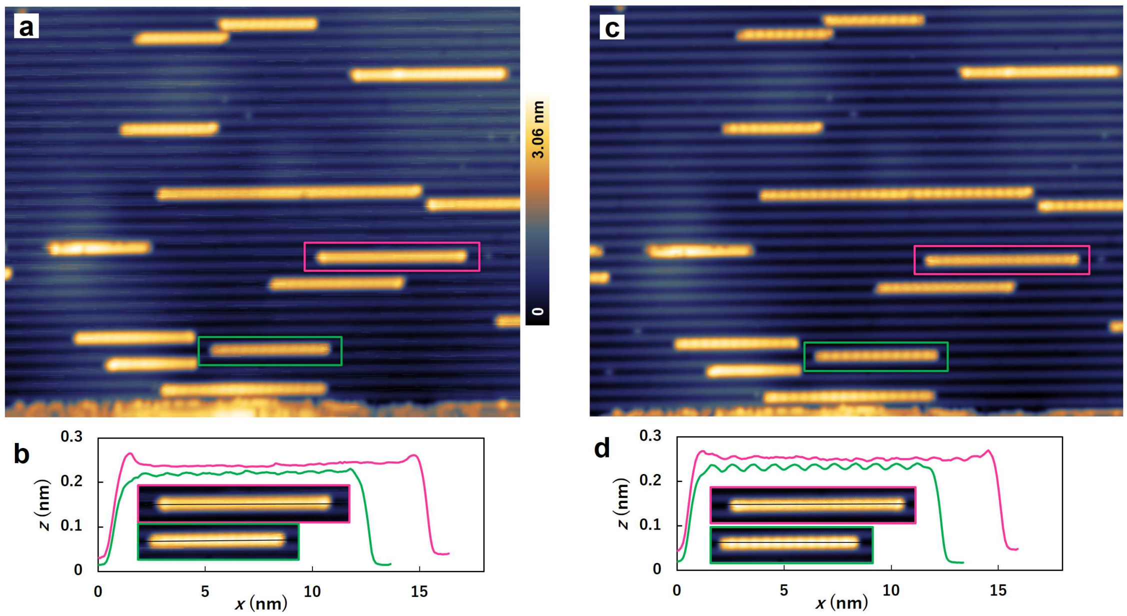

Figure S2: (a) SP-STM topography image of Fe chain on Ir(001). Imaging condition: Constant current mode. $V = 500\,\mathrm{mV}$, $I = 1.0\,\mathrm{nA}$, $T = 4.5\,\mathrm{K}$, $B = -4.0\,\mathrm{T}$. (b) Line profile obtained from two Fe chains in (a). Inset shows the position of the line profile with SP-STM topography image of two Fe chains indicated by different color boxes in (a). (c) SP-STM topography image of Fe chain on Ir(001) obtained at same area as (a). Imaging condition: Constant current mode. $V = 500\,\mathrm{mV}$, $I = 1.0\,\mathrm{nA}$, $T = 4.5\,\mathrm{K}$, $B = -11.0\,\mathrm{T}$. (d) Inset shows the position of the line profile with SP-STM topography image of two Fe chains indicated by different color boxes in (c).

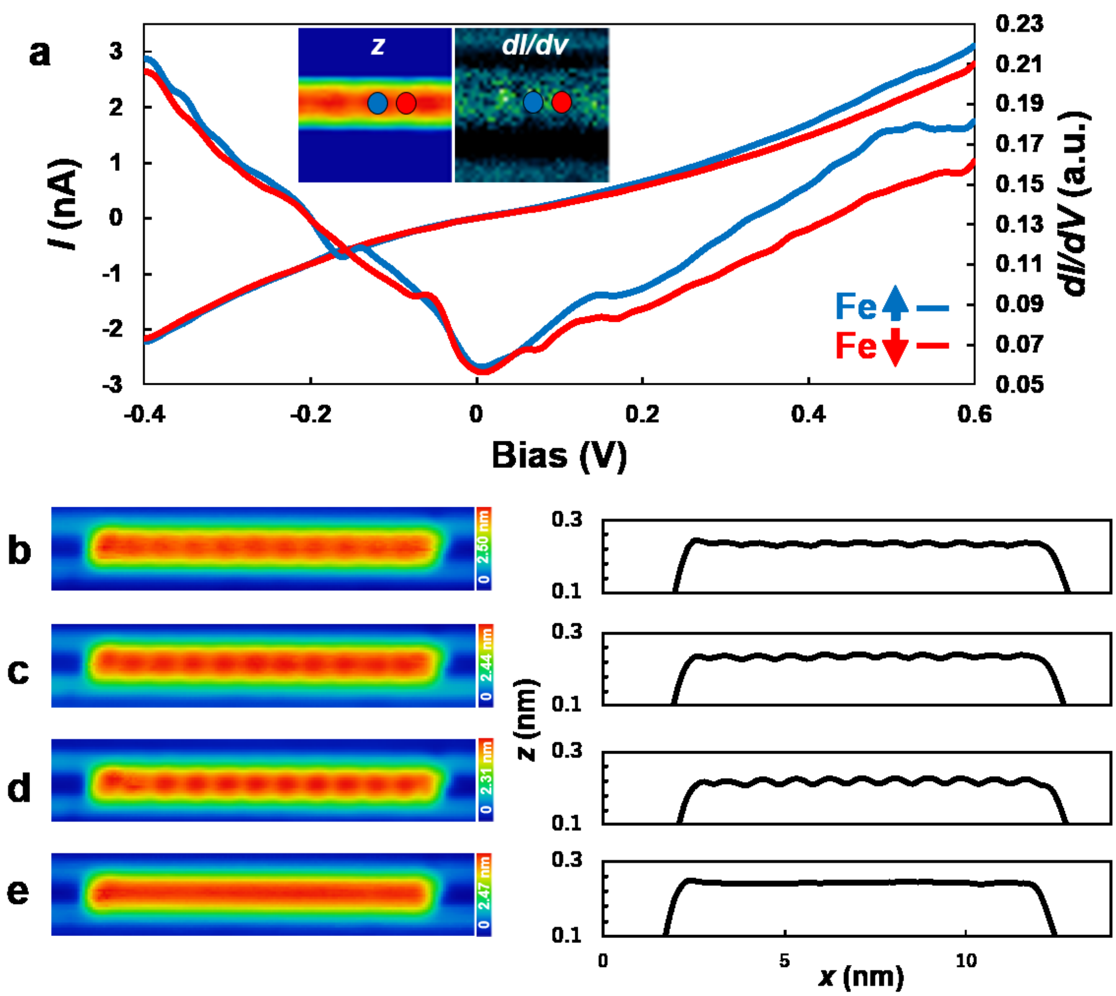

Figure S3: (a) Tunneling current I and $\mathrm{d}I/\mathrm{d}V$ spectra taken on top of maximum spin contrast (blue) and a minimum spin contrast (red) of Fe chain on Ir(001), locations indicated in inset by dots with different colors. (b-e), Consecutive STM topography image and the corresponding line profile of Fe chain on Ir(001). Imaging condition: Constant current mode. $I = 3.0\,\mathrm{nA}$, $T = 4.5\,\mathrm{K}$, $B = 3.0\,\mathrm{T}$, (b) $V = 600\,\mathrm{mV}$; (c) $V = 300\,\mathrm{mV}$; (d) $V = 100\,\mathrm{mV}$; (e) $V = -600\,\mathrm{mV}$.

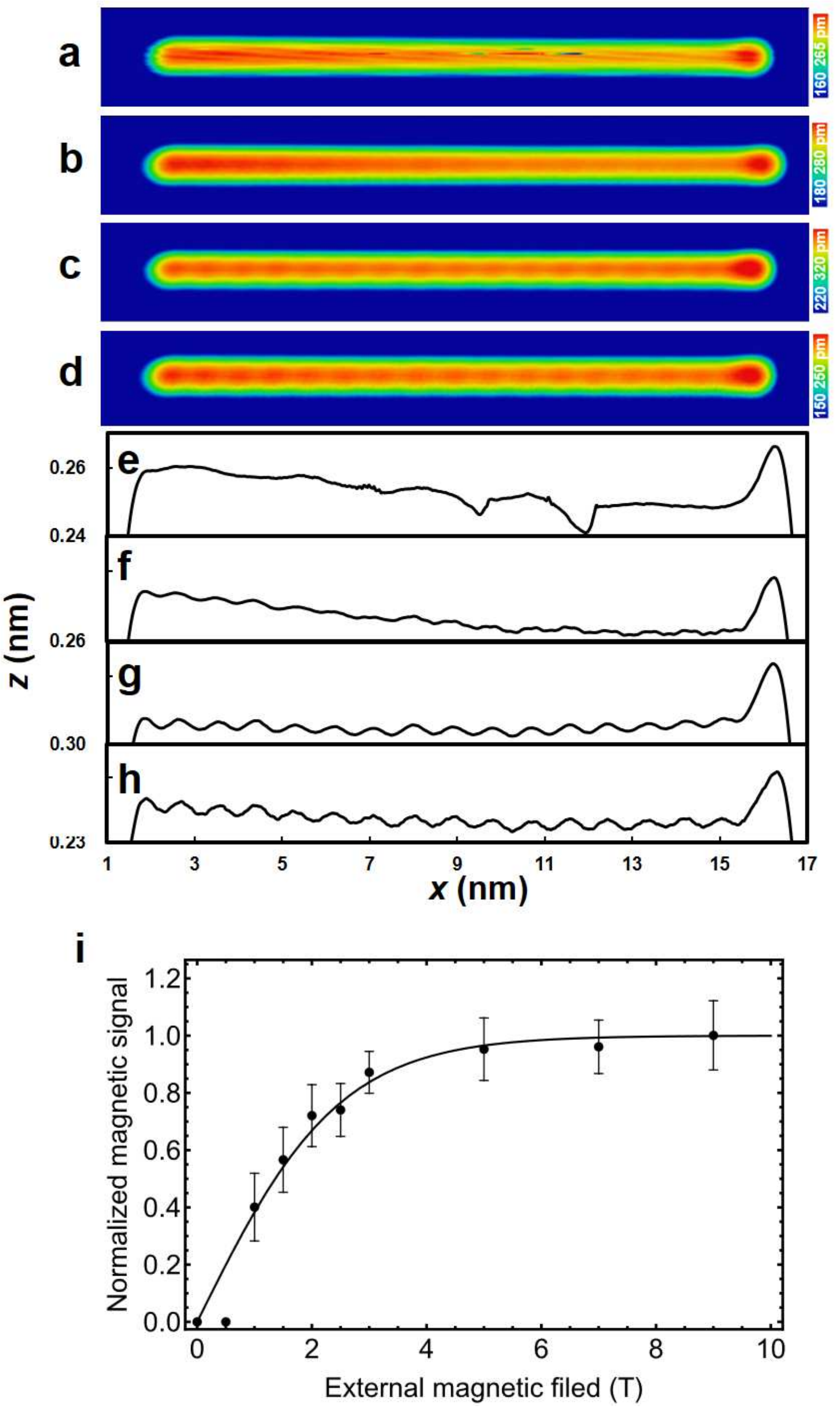

Figure S4: (a-d) Consecutive STM topography image and the corresponding line profile of Fe chain on Ir(001). Imaging condition: Constant current mode. $I = 2.0\,\mathrm{nA}$, $V = 600\,\mathrm{mV}$, $T = 4.5\,\mathrm{K}$, (a) $B = 0.0\,\mathrm{T}$; (b) $B = 1.0\,\mathrm{T}$; (c) $B = 3.0\,\mathrm{T}$; (d) $B = 7.0\,\mathrm{T}$. (e-h) Topographic line profile taken along the chain axis from (a-d). (i), The normalized magnetic corrugation amplitude of Fe chain as a function of the external magnetic field. Error bar indicates standard error.

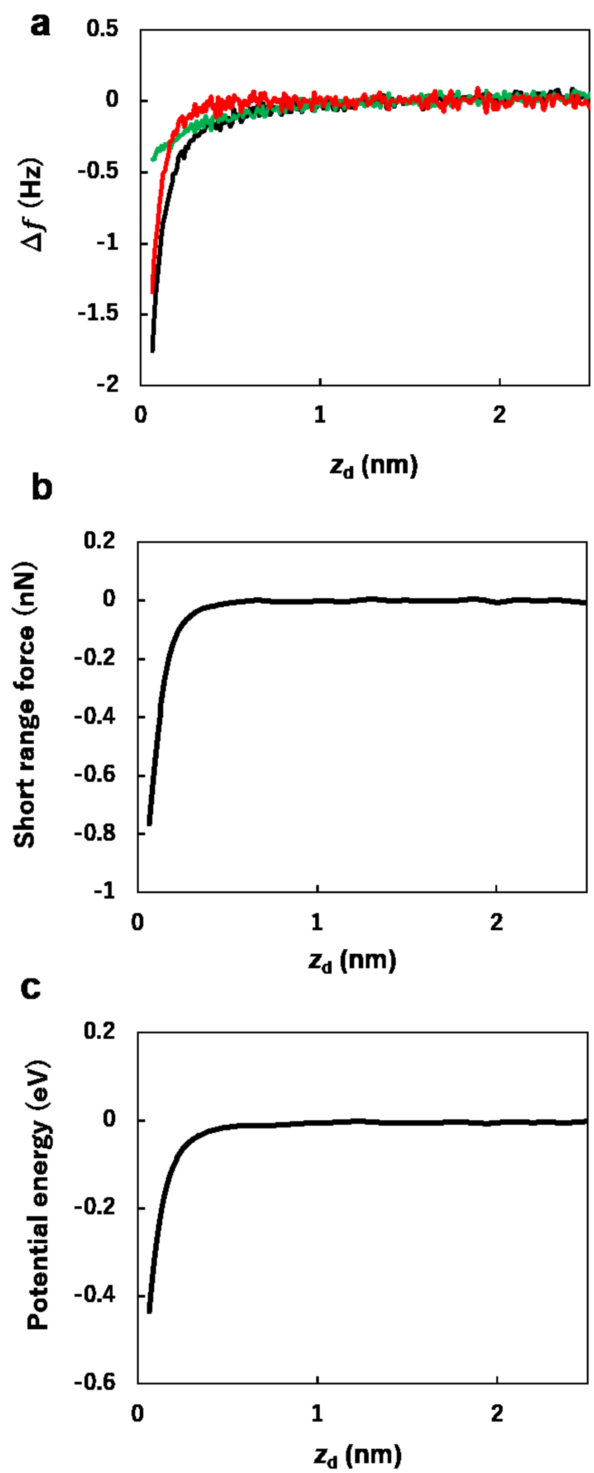

Figure S5: (a) Δf (z_d) spectra taken on top of Fe chain (black $\Delta f_{\mathrm{Fe\,chain}}$ (z_d)), Ir(001) (green Δf_{Ir} (z_d)) and the subtraction of them (red, Δf_{SR} (z_d) = $\Delta f_{\mathrm{Fe\,chain}}$ (z_d) - Δf_{Ir} (z_d)). (b) Short-range force F_{SR} (z_d) obtained from Δf_{SR} (z_d). (c) Potential energy U (z_d) obtained from F_{SR} (z_d).

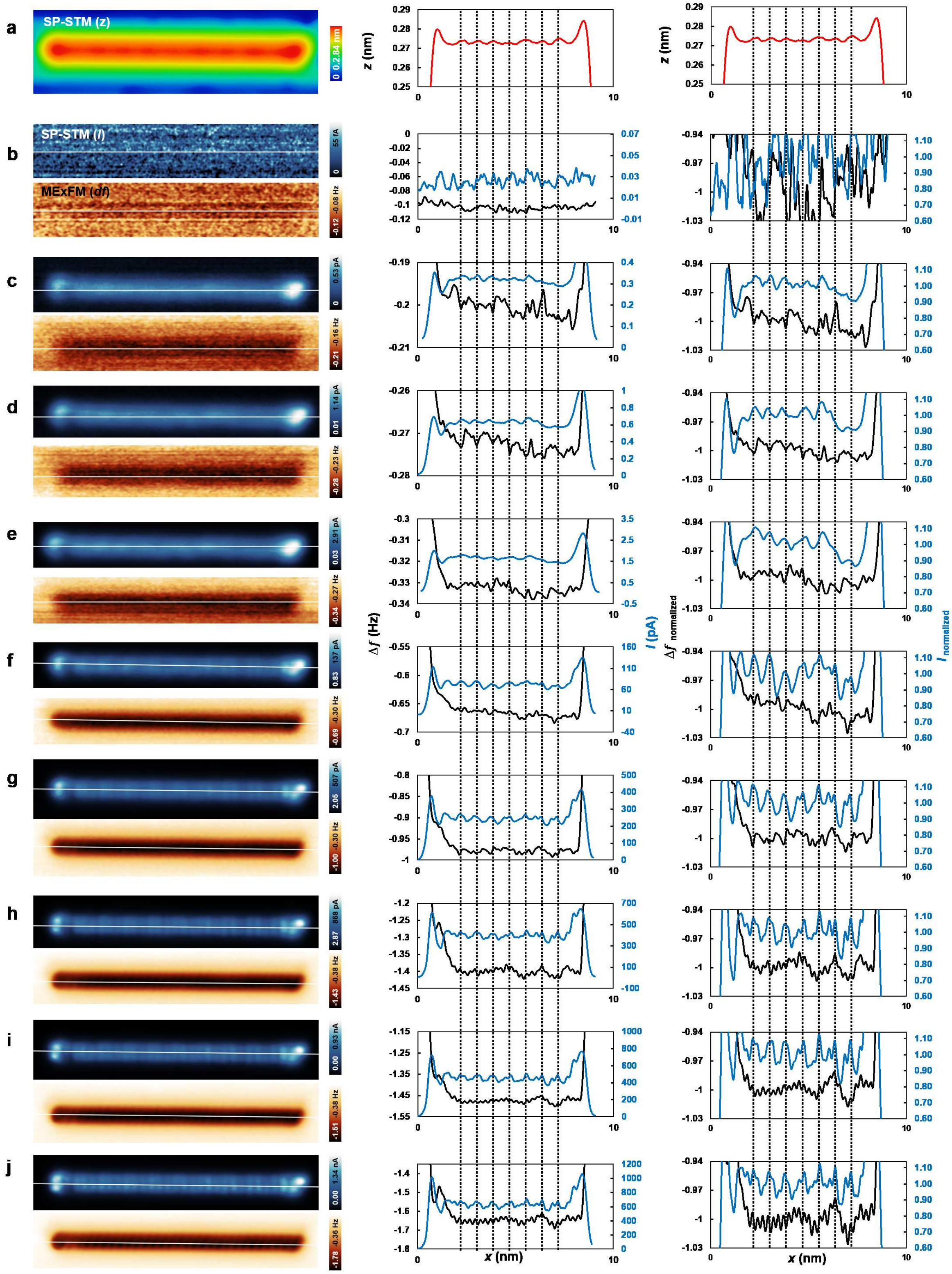

Figure S6: (a) Topographic SP-STM images of Fe chain on Ir(001) with the corresponding line profile. Imaging condition: Constant current mode. $I = 1.5\,\mathrm{nA}$, $V = 600\,\mathrm{mV}$, $T = 4.5\,\mathrm{K}$. This image is same as Figure 3a in the main text. (b-j) Consecutive MExFM and SP-STM images of tunneling current and Δf images of the Fe chain on Ir(001) with the corresponding line profile and the normalized line profiles. Imaging condition: Constant current height, $V = 65\,\mu\mathrm{V}$, $T = 4.5\,\mathrm{K}$, $B = 3.0\,\mathrm{T}$, Tip height (b) $z_\mathrm{d} = 0.544\,\mathrm{nm}$; (c) $z_\mathrm{d} = 0.314\,\mathrm{nm}$; (d) $z_\mathrm{d} = 0.284\,\mathrm{nm}$; (e) $z_\mathrm{d} = 0.194\,\mathrm{nm}$; (f) $z_\mathrm{d} = 0.149\,\mathrm{nm}$; (g) $z_\mathrm{d} = 0.134\,\mathrm{nm}$; (h) $z_\mathrm{d} = 0.079\,\mathrm{nm}$; (i) $z_\mathrm{d} = 0.074\,\mathrm{nm}$; (j) $z_\mathrm{d} = 0.069\,\mathrm{nm}$. Figure 3(b-g) in the main text are same as the tunneling current and Δf images of (d,f,j). Dashed lines across the line profiles indicate the lateral position of maximum of the magnetic contrast in (a).

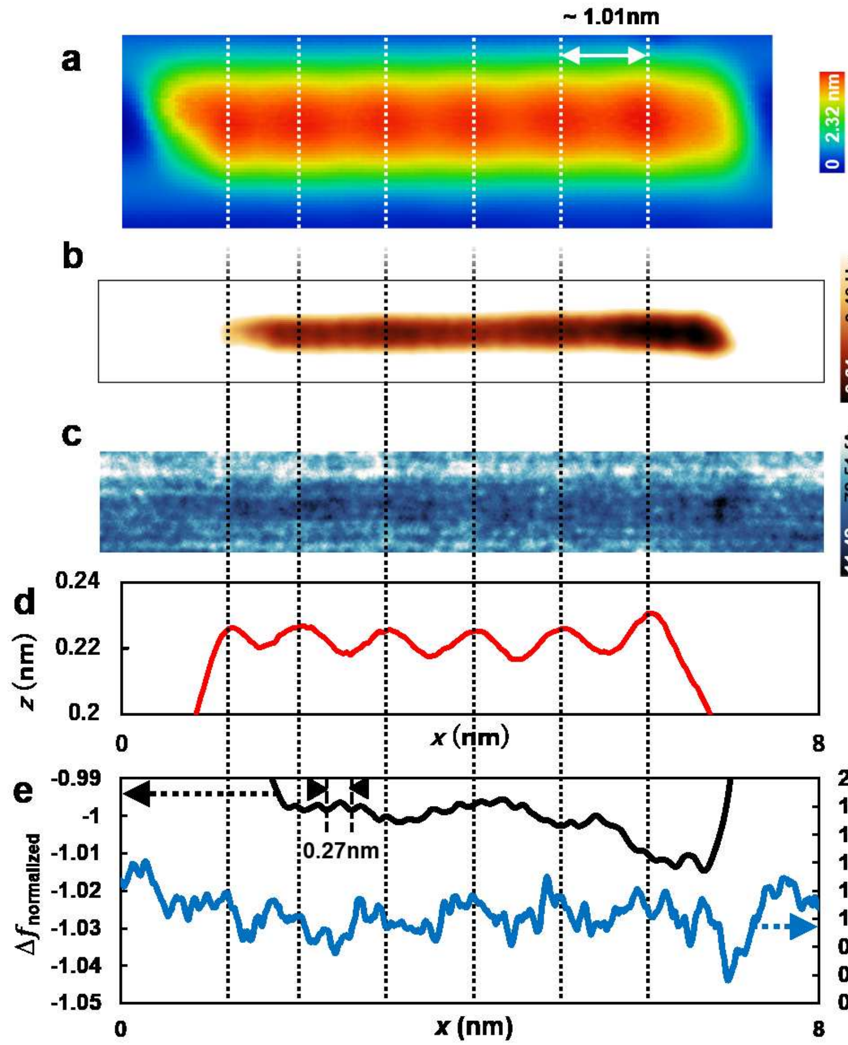

Figure S7: (a) SP-STM topography image of Fe chain on Ir(001). Imaging condition: Constant current mode. $I = 3.0\,\mathrm{nA}$, $V = 500\,\mathrm{mV}$, $T = 4.5\,\mathrm{K}$, $B = 3.0\,\mathrm{T}$. (b,c) MExFM and SP-STM images of Δf and tunneling current images of Fe chain. Imaging condition: Constant height mode, $V = 100\,\mathrm{\mu V}$, $T = 4.5\,\mathrm{K}$, $B = 3.0\,\mathrm{T}$. (d) Line profile obtained from (a). (e) Normalized line profiles obtained from (b, c). The profiles are obtained across the chain axis. Dashed line across the images and the line profile indicates the lateral position of maximum of the magnetic contrast in (d).

References

(S1) Sugimoto, Y.; Onoda, J. Force spectroscopy using a quartz length-extension resonator. *Applied Physics Letters* **2019**, *115*, 173104.

(S2) Menzel, M.; Mokrousov, Y.; Wieser, R.; Bickel, J. E.; Vedmedenko, E.; Blügel, S.; Heinze, S.; von Bergmann, K.; Kubetzka, A.; Wiesendanger, R. Information transfer by vector spin chirality in finite magnetic chains. *Physical review letters* **2012**, *108*, 197204.

(S3) Menzel, M. Non-collinear magnetic ground states observed in iron nanostructures on iridium surfaces. Ph.D. thesis, University of Hamburg, 2011.

(S4) Gilarowski, G.; Méndez, J.; Niehus, H. Initial growth of Cu on Ir(100)-(5×1). *Surface Science* **2000**, *448*, 290–304.

(S5) Hammer, L.; Meier, W.; Schmidt, A.; Heinz, K. Submonolayer iron film growth on reconstructed $\mathrm{Ir}(100) - (5 \times 1)$. *Phys. Rev. B* **2003**, *67*, 125422.

(S6) Menzel, M.; Kubetzka, A.; von Bergmann, K.; Wiesendanger, R. Parity effects in 120 spin spirals. *Physical Review Letters* **2014**, *112*, 047204.

(S7) Onoda, S. Pushing Bits Through a Spin Wire. *Physics* **2012**, *5*, 53.

(S8) Fölsch, S.; Martínez-Blanco, J.; Yang, J.; Kanisawa, K.; Erwin, S. C. Quantum dots with single-atom precision. *Nature nanotechnology* **2014**, *9*, 505–508.

(S9) Sagisaka, K.; Fujita, D. Quasi-one-dimensional quantum well on Si (100) surface crafted by using scanning tunneling microscopy tip. *Applied physics letters* **2006**, *88*.

(S10) von Bergmann, K.; Kubetzka, A.; Pietzsch, O.; Wiesendanger, R. Interface-induced chiral domain walls, spin spirals and skyrmions revealed by spin-polarized scanning tunneling microscopy. *Journal of Physics: Condensed Matter* **2014**, *26*, 394002.

(S11) Sader, J. E.; Jarvis, S. P. Accurate formulas for interaction force and energy in frequency modulation force spectroscopy. *Applied physics letters* **2004**, *84*, 1801–1803.

(S12) Mazzarello, R.; Tosatti, E. Connection between magnetism and structure in Fe double chains on the Ir(100) surface. *Phys. Rev. B* **2009**, *79*, 134402.

(S13) Grenz, J.; Köhler, A.; Schwarz, A.; Wiesendanger, R. Probing the Nano-Skyrmion Lattice on Fe/Ir(111) with Magnetic Exchange Force Microscopy. *Phys. Rev. Lett.* **2017**, *119*, 047205.